Wave-equation migration velocity analysis by inversion of differential image perturbations

Paul Sava* and Biondo Biondi, Stanford University

SUMMARY

Wave-equation migration velocity analysis is based on the linear relation that can be established between a perturbation in the migrated image and the corresponding perturbation in the slowness function. Our method formulates an objective function in the image space, in contrast with other wave-equation tomography techniques which formulate objective functions in the data space. We iteratively update the slowness function to account for improvements in the focusing quality of the migrated image. Wave-equation migration velocity analysis (WEMVA) produces wrong results if it starts from an image perturbation which is not compliant with the assumed Born approximation. Other attempts to correct this problem lead to either unreliable or hard to implement solutions. We overcome the major limitation of the Born approximation by creating image perturbations consistent with this approximation. Our image perturbation operator is computed as a derivative of prestack Stolt residual migration, thus our method directly exploits the power of prestack residual migration in migration velocity analysis.

INTRODUCTION

Migration velocity analysis based on downward continuation methods, also known as *wave-equation migration velocity analysis*, is a technique designed as a companion to wave-equation migration (Biondi and Sava, 1999; Sava and Fomel, 2002). The main idea of WEMVA is to use downward continuation operators for migration velocity analysis (MVA), as well as for migration. This is in contrast with other techniques which use downward continuation for migration, but traveltime-based techniques for migration velocity analysis (Clapp, 2001; Liu et al., 2001; Mosher et al., 2001).

WEMVA is closer to conventional MVA than other wave-equation tomography methods (Noble et al., 1991; Bunks et al., 1995; Forgues et al., 1998) because it tries to maximize the quality of the migrated image instead of trying to match the recorded data. In this respect, our method is related to Differential Semblance Optimization (Symes and Carazzone, 1991) and Multiple Migration Fitting (Chavent and Jacewitz, 1995). However, with respect to these two methods, our method has the advantage of exploiting the power of residual prestack migration to speed up the convergence, and it also gives us the ability to guide the inversion by geologic interpretation.

WEMVA benefits from the same advantages over traveltime estimation methods as wave-equation migration benefits over Kirchhoff migration. The most important among them are the accurate handling of complex wavefields which are characterized by multipathing, and the band-limited nature of the imaging process, which can handle sharp velocity variations much better than traveltime-based methods (Woodward, 1992). Complex geology, therefore, is where WEMVA is expected to provide the largest benefits.

WEMVA is based on a linearization of the downward-continuation operator using the Born approximation. This approximation leads to severe limitations on the magnitude and size of the anomalies that can be handled. It, therefore, cannot operate successfully exactly in the regions of highest complexity. Other methods of linearization are possible (Sava and Fomel, 2002), but neither one allows for arbitrarily large anomalies.

In our early tests (Biondi and Sava, 1999), we construct the image perturbation using Prestack Stolt Residual Migration (PSRM) (Sava, 2000). In summary, this residual migration method provides updated images for new velocity maps that correspond to a fixed ratio (ρ) of the new velocity with respect to the original velocity map. Residual migration is run for various ratio parameters, and finally we pick the best image by selecting the flattest gathers at every point.

The main disadvantage of building the image perturbation using PSRM is that, for large velocity ratio parameters (ρ), the background and improved images can get more than $\pi/4$ out of phase. Therefore, the image perturbation computed by the forward operator and the one computed by residual migration are fundamentally different, and can have contradictory behaviors when using the Born-linearized WEMVA operator for inversion.

Alternative methods can be used to create image perturbations for WEMVA, in compliance with the Born approximation and computed directly from the background image. We present an analytic differential procedure starting from the background image and leading to image perturbations similar to the ones created using the forward WEMVA operator.

We begin with a discussion of scattering theory in the context of wavefield extrapolation, followed by a brief description of the method we use to create differential image perturbations, and a synthetic example.

For all our examples, we migrate data using wavefield extrapolation techniques. We present the images decomposed in components proportional to the reflection magnitude for various incidence angles at the reflector, commonly referred to as angle-domain common image gathers (Weglein and Stolt, 1999; Sava and Fomel, 2003; Rickett and Sava, 2001).

WAVEFIELD SCATTERING

In migration by downward continuation, the wavefield at depth $z + \Delta z$, $\mathcal{W}(z + \Delta z)$, is obtained by phase-shift from the wavefield at depth z, $\mathcal{W}(z)$:

$$\mathcal{W}(z + \Delta z) = \mathcal{W}(z)e^{-ik_z \Delta z}. \quad (1)$$

Using a Taylor series expansion, the depth wavenumber (k_z) depends linearly on its value in the reference medium (k_{z_o}) and the laterally varying slowness $s(x, y, z)$ in the depth interval under consideration

$$k_z \approx k_{z_o} + \left. \frac{dk_z}{ds} \right|_{s=s_o} (s - s_o). \quad (2)$$

s_o represents the constant slowness associated with the depth slab between the two depth intervals. $\left. \frac{dk_z}{ds} \right|_{s=s_o}$ represents the derivative of the depth wavenumber with respect to the reference slowness and can be implemented in many different ways, e.g by the Fourier-domain method of Huang et al. (1999).

The wavefield downward continued through the *background* slowness $s_b(x, y, z)$ is

$$\mathcal{W}_b(z + \Delta z) = \mathcal{W}(z)e^{-i\left[k_{z_o} + \left. \frac{dk_z}{ds} \right|_{s=s_o} (s_b - s_o) \right] \Delta z}, \quad (3)$$

and the full wavefield $\mathcal{W}(z + \Delta z)$ depends on the background wavefield $\mathcal{W}_b(z + \Delta z)$ by

$$\mathcal{W}(z + \Delta z) = \mathcal{W}_b(z + \Delta z)e^{-i \left. \frac{dk_z}{ds} \right|_{s=s_o} \Delta s \Delta z}, \quad (4)$$
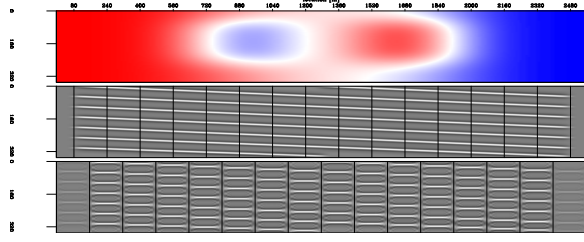
Figure 1: Correct model: slowness (top), stacked image (middle) and selected angle-gathers (bottom).

Figure 2: Background model for WEMVA: slowness (top), stacked image (middle) and selected angle-gathers (bottom).

where Δs represents the difference between the true and background slownesses $\Delta s = s - s_b$.

Defining the *wavefield perturbation* $\Delta W (z + \Delta z)$ as the difference between the wavefield propagated through the medium with correct velocity, $W(z + \Delta z)$, and the wavefield propagated through the background medium, $W_b(z + \Delta z)$, we can write

$$
\begin{aligned}
\Delta W(z + \Delta z) &= W(z + \Delta z) - W_b(z + \Delta z) \quad (5) \\
&= W_b(z + \Delta z) \left[e^{-i \frac{dk_z}{ds}\big|_{s=s_o} \Delta s \Delta z} - 1 \right]. \quad (6)
\end{aligned}
$$

Equation (5) represents the foundation of the wave-equation migration velocity analysis method. One major problem with Equation (5) is that the wavefield ΔW and slowness perturbations Δs are not linearly related. For inversion purposes, we need to find a linearization of this equation around the reference slowness, s_o. Biondi and Sava (1999) linearize Equation (5) using the Born approximation ($e^{i\phi} \approx 1 + i\phi$). With this choice, the WEMVA Equation (5) becomes

$$
\Delta W(z + \Delta z) = W_b(z + \Delta z) \left[-i \frac{dk_z}{ds}\bigg|_{s=s_o} \Delta s \Delta z \right]. \quad (7)
$$

The wavefield perturbation ΔW in Equation (7) turns into an image perturbation $\Delta \mathcal{R}$ after we apply an imaging condition, e.g. summation over frequencies. The WEMVA objective function is

$$
\min_{\Delta s} \| \Delta \mathcal{R} - \mathbf{L} \Delta s \| \quad (8)
$$

where $\mathbf{L}$ is a linear operator defined recursively from Equation (7) at every depth level and frequency. We estimate the slowness update by minimizing this objective function through an iterative conjugate gradient optimization technique.

DIFFERENTIAL IMAGE PERTURBATION

Residual migration can be used to create image perturbations ($\Delta \mathcal{R}$). In its simplest form, we can build $\Delta \mathcal{R}$ as a difference between an *improved* image ($\mathcal{R}$) and the *reference* image ($\mathcal{R}_b$)

$$
\Delta \mathcal{R} = \mathcal{R} - \mathcal{R}_b, \quad (9)
$$

where $\mathcal{R}$ is derived from $\mathcal{R}_b$ as a function of the parameter ρ, which is the ratio of the original and improved velocities. Of course, the improved velocity map is unknown explicitly, but it is described indirectly by the ratio map of the two velocities.

If we denote by 1 the velocity ratio that corresponds to the background velocity model and define $\Delta \rho = \rho - 1$, we can also write the discrete version of the image perturbation as

$$
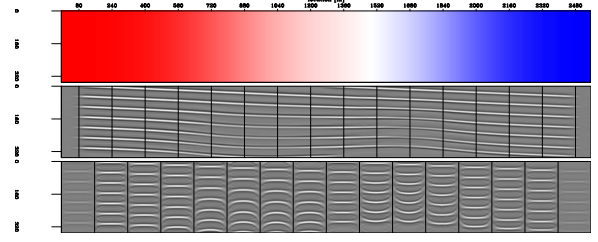\Delta \mathcal{R} \approx \frac{\mathcal{R} - \mathcal{R}_b}{\rho - 1} \Delta \rho, \quad (10)
$$

equation which can also be written in differential form as

$$
\Delta \mathcal{R} \approx \frac{d\mathcal{R}}{d\rho}\bigg|_{\rho=1} \Delta \rho, \quad (11)
$$

or, equivalently, using the chain rule, as

$$
\Delta \mathcal{R} \approx \frac{d\mathcal{R}}{dk_z} \frac{dk_z}{d\rho}\bigg|_{\rho=1} \Delta \rho, \quad (12)
$$

where k_z is the depth wavenumber defined for PSRM.

Equation (12) offers the possibility to build the image perturbation directly. We achieve this by computing three elements: the derivative of the image with respect to the depth wavenumber, and two weighting functions, one for the derivative of the depth wavenumber with respect to the velocity ratio parameter (ρ), and the other one for the magnitude of the $\Delta \rho$ perturbation from the reference to the improved image.

Firstly, the image derivative in the Fourier domain, $\frac{d\mathcal{R}}{dk_z}$, is straightforward to compute in the space domain as

$$
\frac{d\mathcal{R}}{dk_z}\bigg|_{\rho=1} = -iz\mathcal{R}_b. \quad (13)
$$

The derivative image is nothing but the imaginary part of the migrated image, scaled by depth.

Secondly, we can obtain the weighting representing the derivative of the depth wavenumber with respect to the velocity ratio parameter, $\frac{dk_z}{d\rho}\big|_{\rho=1}$, starting from the double square root (DSR) equation written for prestack Stolt residual migration (Sava, 2000):

$$
\begin{aligned}
k_z &= k_{zs} + k_{zr} \\
&= \frac{1}{2}\sqrt{\rho^2 \mu^2 - |\mathbf{k}_s|^2} + \frac{1}{2}\sqrt{\rho^2 \mu^2 - |\mathbf{k}_r|^2},
\end{aligned}
$$

where μ is given by the expression:

$$
\mu^2 = \frac{\left[4\left(k_{zo}\right)^2 + (|\mathbf{k}_r| - |\mathbf{k}_s|)^2 \right]\left[4\left(k_{zo}\right)^2 + (|\mathbf{k}_r| + |\mathbf{k}_s|)^2 \right]}{16\left(k_{zo}\right)^2}, \quad (14)
$$

$\left(k_{zs}, k_{zr}\right)$ are the depth wavenumbers and ($|\mathbf{k}_s|, |\mathbf{k}_r|$) are the spatial wavenumbers for the sources and receivers, respectively.

The derivative of k_z with respect to ρ is

$$
\frac{dk_z}{d\rho} = \rho \left(\frac{\mu^2}{4k_{zs}} + \frac{\mu^2}{4k_{zr}} \right), \quad (15)
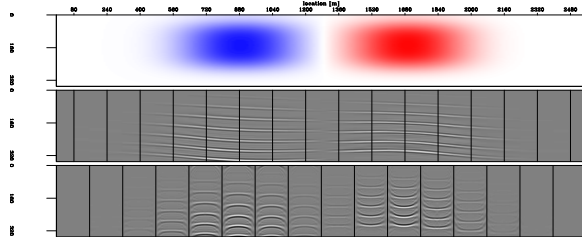$$

Figure 3: Image perturbation by the forward WEMVA operator: slowness perturbation (top), stacked image (middle) and selected angle-gathers (bottom).

Figure 4: Difference image perturbation: inverted slowness perturbation (top), stacked image (middle) and selected angle-gathers (bottom).

therefore

$$\left.\frac{dk_z}{d\rho}\right|_{\rho=1} = \frac{\mu^2}{2\sqrt{\mu^2 - |\mathbf{k}_s|^2}} + \frac{\mu^2}{2\sqrt{\mu^2 - |\mathbf{k}_r|^2}}. \qquad (16)$$

Finally, $\Delta\rho$ can be picked from the set of residually migrated images at various values of the parameter ρ (Sava, 2000). One criterion that could be used to estimate $\Delta\rho$ is the flatness of the angle-domain image gathers, which can be measured through derived parameters, such as stack power, semblance or differential semblance.

EXAMPLE

We demonstrate the method on a synthetic example consisting of several dipping reflectors embedded in laterally varying slowness. Figure 1 shows from top to bottom the correct slowness model, the stacked reflectivity model and a few selected angle-gathers. We use this model to create a synthetic dataset.

Figure 2 shows from top to bottom the background slowness model, the stacked reflectivity and a few selected angle-gathers. Since we do not use the correct slowness, the angle gathers are not flat and the image is distorted.

Figure 3 shows from top to bottom the slowness perturbation between the true and the background slowness models, and the image perturbation created using the forward linear WEMVA operator: the stacked image in the middle panel and a few selected angle-gathers (bottom). This image is, by definition, consistent with the Born approximation. In practice, however, we need to go backward and compute a slowness perturbation from an image perturbation.

The problem with the Born approximation is illustrated in Figure 4. The image perturbation obtained as a difference between the background image and an improved version of it is presented in the bottom two panels. The phase difference between corresponding events is larger than a fraction of the wavelet, and clearly violates the Born approximation. The inverted slowness anomaly (top panel) shows the characteristic sign changes usually seen in wave-equation tomography when the limits of the Born approximation are violated.

Figure 5 illustrates our method for computing the image perturbation from the background data. We run residual migration as indicated in the preceding section and then pick at every location in the image the best velocity ratio ρ which corresponds to flat gathers. We also compute and image derivative according to Equation (12) without the $\Delta\rho$ scaling. Figure 5 shows the stacked image derivative and a few selected angle-gathers. The shape of this image is similar to that of the background image, with some phase and amplitude differences introduced by the derivative process.
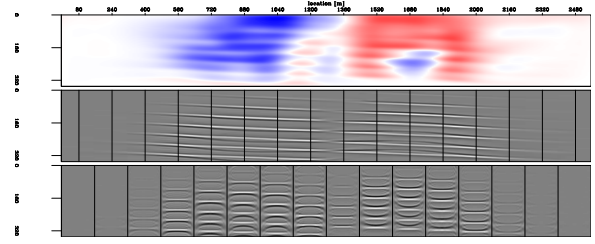
We use Equation (12) and the $\Delta\rho$ weight (Figure 5) to create the differential image perturbation (Figure 6). This image perturbation is comparable in shape and magnitude with the ideal perturbation (Figure 3). This indicates that we have succeeded to compute from the background image an image perturbation which is consistent with the Born approximation, and, therefore, we can use the linearized WEMVA operator without the danger of divergence due to images going out of phase.

For comparison, Figure 7 shows, from top to bottom, the image perturbations computed with the forward WEMVA operator, the one computed as a simple difference between the background image and an improved version of it, and the one computed by our differential procedure. We observe in the middle panel events which are largely out of phase, indicating that we cannot use the Born linearization. In contrast, the differential image perturbation is fully consistent with the one computed by the forward operator.

We use the image perturbation depicted in the bottom two panels of Figure 6 to invert for the corresponding slowness perturbation. We use 10 linear iterations for this example, with only one non-linear iteration.

Finally, Figure 8 shows from top to bottom the updated slowness model, and the updated staked image in the middle panel and a few selected angle-gathers in the bottom panel, which are much flatter than the ones of the background image (Figure 2).

CONCLUSIONS

We present an extension of our recursive wave-equation migration velocity analysis method operating in the image domain. Our method is based on the linearization of the downward continuation operator that relates perturbations in slowness to perturbations in image. The fundamental idea is to improve the quality of the slowness function by optimizing the focusing of the migrated image,
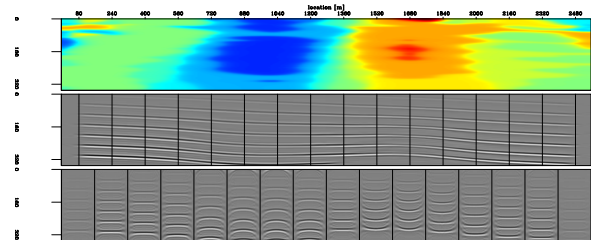

Figure 5: Differential image perturbation: picked $\Delta\rho$ map (top), stacked image differential (middle) and selected angle-gathers (bottom).
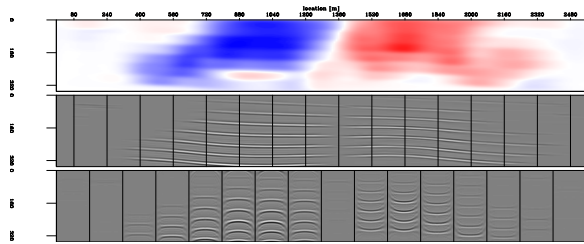
Figure 6: Differential image perturbation: inverted slowness perturbation (top), stacked image (middle) and selected angle-gathers (bottom).

Figure 8: Estimated model after WEMVA: slowness (top), stacked image (middle) and selected angle-gathers (bottom).

and not by fitting the data recorded at the surface directly.

We construct the image perturbations by a differential operator applied to the reference image. In this way, we ensure that we do not violate the inherent Born approximation made in our method. This method directly constructs the image perturbation from the background image, and is always compliant with the Born approximation which is the underlying assumption of WEMVA. We show that we can obtain slowness anomalies that are fully consistent with those obtained by the application of the forward and adjoint WEMVA operators.

REFERENCES

Biondi, B., and Sava, P., 1999, Wave-equation migration velocity analysis: 69th Ann. Internat. Meeting, Soc. Expl. Geophys., Expanded Abstracts, 1723–1726.

Bunks, C., Saleck, F. M., Zaleski, S., and Chavent, G., 1995, Multiscale seismic waveform inversion: Geophysics, **60**, no. 05, 1457–1473.

Chavent, G., and Jacewitz, C. A., 1995, Determination of background velocities by multiple migration fitting: Geophysics, **60**, no. 02, 476–490.

Clapp, R. G., 2001, Geologically constrained migration velocity analysis: Ph.D. thesis, Stanford University.

Forgues, E., Scala, E., and Pratt, R. G., 1998, High resolution velocity model estimation from refraction and reflection data: 68th Ann. Internat. Mtg, Soc. Expl. Geophys., Expanded Abstracts, 1211–1214.
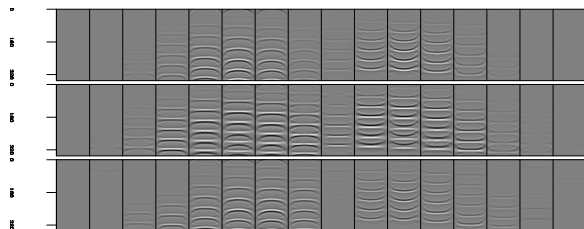
Figure 7: Image perturbation comparison: image perturbation computed by the forward WEMVA operator (top), image perturbation computed as a difference between the background image and a residually migrated one, which violates the Born approximation (middle), image perturbation computed by our differential method (bottom).
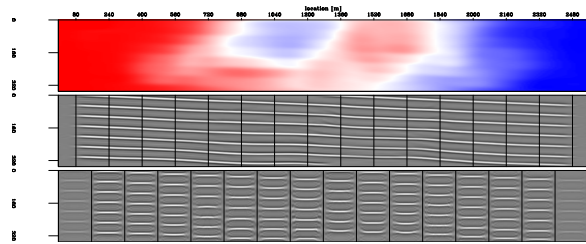
Huang, L., Fehler, M. C., and Wu, R. S., 1999, Extended local Born Fourier migration method: Geophysics, **64**, no. 5, 1524–1534.

Liu, W., Popovici, A., Bevc, D., and Biondi, B., 2001, 3-D migration velocity analysis for common image gathers in the reflection angle domain: 71st Annual Internat. Mtg., Soc. Expl. Geophys., Expanded Abstracts, 885–888.

Mosher, C., Jin, S., and Foster, D., 2001, Migration velocity analysis using angle image gathers: 71st Annual Internat. Mtg., Soc. Expl. Geophys., Expanded Abstracts, 889–892.

Noble, M., Lindgren, J., and Tarantola, A., 1991, Large-sized, nonlinear inversion of a marine data set: Retrieving the source, the background velocity and the impedance contrasts: 61st Ann. Internat. Mtg, Soc. Expl. Geophys., Expanded Abstracts, 893–896.

Rickett, J., and Sava, P., 2001, Offset and angle domain common-image gathers for shot-profile migration: 71st Ann. Internat. Meeting, Soc. Expl. Geophys., Expanded Abstracts, 1115–1118.

Sava, P., and Fomel, S., 2002, Wave-equation migration velocity analysis beyond the Born approximation: 72nd Ann. Internat. Mtg., Soc. Expl. Geophys., Expanded Abstracts, 2285–2288.

Sava, P., and Fomel, S., 2003, Angle-domain common-image gathers by wavefield continuation methods: Geophysics, **68**, in press.

Sava, P., 2000, Prestack Stolt residual migration for migration velocity analysis: 70th Ann. Internat. Mtg., Soc. Expl. Geophys., Expanded Abstracts, 992–995.

Symes, W. W., and Carazzone, J. J., 1991, Velocity inversion by differential semblance optimization: Geophysics, **56**, no. 05, 654–663.

Weglein, A., and Stolt, R., 1999, Migration-inversion revisited: The Leading Edge, **18**, 950–952.

Woodward, M. J., 1992, Wave-equation tomography: Geophysics, **57**, no. 01, 15–26.